This article has been accepted for publication in a future issue of this journal, but has not been fully edited. Content may change prior to final publication. Citation information: DOI 10.1109/TSG.2018.2825322, IEEE Transactions on Smart Grid

Coordinated Power Control of Electric Vehicles for Grid Frequency Support: MILP-based Hierarchical Control Design

Kuljeet Kaur, *Student Member, IEEE,* Neeraj Kumar, *Senior Member, IEEE,* and Mukesh Singh, *Member, IEEE*

Abstract—Frequency regulation is one of the most crucial ancillary services that strives to maintain the demand and supply in Smart Grid (SG) setup. The deviations in grid's frequency can be managed efficiently by adjusting the power generation and consumption of supply and demand sides respectively. Traditionally, frequency support is provided using conventional generators but their usage leads to the emission of harmful gases, degraded heat rate, and associated wear and tear. However, Electric Vehicles (EVs) can play a significant role in managing demand and supply imbalances in the near future; with their penetration expected to reach 400 billion by 2020. Moreover, EVs have large charging and discharging capacities due to which they can provide instantaneous frequency support. Motivated by these factors, in this paper, a power management scheme has been presented to leverage the participation of EVs for Secondary Frequency Regulation (SFR). The proposed scheme uses a 2-level hierarchical control mechanism to attain the following objectives: (i) to minimize the frequency deviations at the grid level, (ii) to support bi-directional Vehicle-to-Grid (V2G) in accordance with users' power requirements, (iii) to generate an optimal schedule for EV's charging and discharging needs, (iv) to reduce battery degradation, and (v) to maximize EV's revenue. Using these objectives, the problem of frequency support has been formulated as a *"Mixed Integer Linear Programming (MILP)"* problem. The proposed scheme has been evaluated using Mosek solver on real-time data acquired from *PJM* and *CAISO*. The results obtained demonstrate the effectiveness of the proposed scheme for providing frequency support in comparison to the existing scheme.

Index Terms—Ancillary services, Electric Vehicles (EVs), Frequency support, Hierarchical control design, Mixed Integer Linear Programming (MILP), Scheduling policy, and Vehicle-to-Grid (V2G).

NOMENCLATURE

AG_i	i^{th} AG under reference
CS_{ij}	j^{th} CS under the control of i^{th} AG
C_{optmax}	Maximum optimal limit for EV's charging rate
C_{optmin}	Minimum optimal limit for EV's charging rate
C_{max}	Maximum suboptimal limit for EV's charging rate
C_{min}	Minimum suboptimal limit for EV's charging rate
$C_{ij}^{sch}(t)$	Scheduled charging rate of the EVs available at the j^{th} CS of the i^{th} AG, at time t
D_{optmax}	Maximum optimal limit for EV's discharging rate
D_{optmin}	Minimum optimal limit for EV's discharging rate
D_{max}	Maximum suboptimal limit for EV's discharging rate
D_{min}	Minimum suboptimal limit for EV's discharging rate
$D_{ij}^{sch}(t)$	Scheduled discharging rate of the EVs available at the j^{th} CS of the i^{th} AG, at time t
E_{ijk}^{rated}	Energy rated capacity of the k^{th} EV
$\mathbb{F}$	Overall objective function
$\mathbb{F}_1$	Objective function for minimizing frequency deviations
$\mathbb{F}_2$	Objective function to maximally support V2G services in terms of charging
$\mathbb{F}_3$	Objective function to maximally support V2G services in terms of discharging
$\mathbb{F}_4$	Objective function for optimal regulation signal dispatch among AGs and CSs
$\mathbb{F}_5$	Objective function for maximizing EV's revenue in SFR
$\mathfrak{F}_i^{down}(t)$	FRC of the i^{th} AG providing regulation down services at time t
$\mathfrak{F}_{ij}^{down}(t)$	FRC of the j^{th} CS providing regulation down services at time t
$\mathfrak{F}_{ijk}^{down}(t)$	FRC of the k^{th} EV providing regulation down services at time t
$\mathfrak{F}_i^{up}(t)$	FRC of the i^{th} AG providing regulation up services at time t
$\mathfrak{F}_{ij}^{up}(t)$	FRC of the j^{th} CS providing regulation up services at time t
$\mathfrak{F}_{ijk}^{up}(t)$	FRC of the k^{th} EV providing regulation up

- *K. Kaur and N. Kumar are with the Department of Computer Science & Engineering, Thapar University, Patiala (Punjab), India. E-mail: kuljeet0389@gmail.com and neeraj.kumar@thapar.edu*
- *M. Singh is with the Department of Electrical & Instrumentation Engineering, Thapar University, Patiala (Punjab), India. E-mail: mukesh.singh@thapar.edu*

This article has been accepted for publication in a future issue of this journal, but has not been fully edited. Content may change prior to final publication. Citation information: DOI 10.1109/TSG.2018.2825322, IEEE Transactions on Smart Grid

	services at time t
$\mathfrak{F}^{tot}(t)$	Total FRC of the V2G setup at time t
i	Index for referring an AG
j	Index for referring a CS
k	Index for referring an EV
$\mathcal{M}$	Number of AGs
$\mathcal{N}$	Number of CSs
$\mathfrak{Pr}^{up}(t)$	Regulation up price at time t
$\mathfrak{Pr}^{down}(t)$	Regulation down price at time t
$\mathfrak{R}^{ref}(t)$	Reference signal generated at t
$\mathfrak{R}_{ij}^{ref,sch}(t)$	Scheduled reference signal for the j^{th} CS at t
$\mathfrak{R}_{i}^{ref,sch}(t)$	Scheduled reference signal for the i^{th} AG at t
SoC	State of Charge
$SoC_{ijk}^{cur}(t)$	Current SoC of the k^{th} EV at t
SoC_{max}	Maximum suboptimal SoC limit upto which an EV can be charged
SoC_{min}	Minimum suboptimal SoC limit upto which an EV can be discharged
SoC_{optmax}	Maximum optimal SoC limit upto which an EV can be charged
SoC_{optmin}	Minimum optimal SoC limit upto which an EV can be discharged
t	Index for referring a time instance
T	Time horizon under reference

1 Introduction

Frequency regulation is an effective mechanism to maintain demand and supply balance in Smart Grid (SG) environment. Even the minute deviations in grid's frequency can trigger significant disturbances in the form of blackouts, brownouts and voltage fluctuations [1]. Hence, in order to effectively manage these deviations, power generation and consumption of respective supply and demand sides need to be adjusted in real-time. Traditionally, frequency support is provided using conventional generators (at the supply side) powered by non-renewable sources of energy. However, use of generators lead to the loss of opportunity to generate additional power, that would otherwise be available to cater the growing energy demands [1], [2]. On the contrary, modern frequency regulation agents such as-commercial buildings, aggregated residential loads and energy storage devices provide more environmental friendly means of frequency support at the demand side. Nevertheless, these agents also suffer from certain drawbacks such as-heavy installation cost of energy storage devices and huge energy waste to facilitate the Heating, Ventilation, Air Conditioning (HVAC) in commercial buildings.

More recently, Electric Vehicles (EVs) have been identified as the major frequency regulation agents (at the demand side) due to their inherent ability to provide instantaneous frequency support [1], [3], [4]. This can be credited to their aggregated Frequency Regulation Capacities (FRCs) which can be effectively utilized to track the Automatic Generation Control (AGC) signal. Additionally, they remain idle for almost 96% of the time which makes them suitable agents for effective frequency support. According to the survey conducted by International Energy Agency, the proportion of EVs has already exceeded the one million count globally [5]. Also, their penetration in the world market is estimated to reach 400 billion by 2020 [5]. Nonetheless, the future penetration of EVs on large scale, may trigger several unseen challenges for the power grids. For example, the increased dependence on electricity to accommodate EV's transportation needs, would emerge as one of the foremost concerns. Additionally, unregulated charging of widely dispersed EVs may affect the grid's stability adversely. Hence, to cater these challenges, Kempton and Letendre introduced the novel concept of Vehicle-to-Grid (V2G) in the year 1997 [6]. The central ideology behind this technology was to support bi-directional energy exchanges between SG and EVs. This capability makes them suitable to be efficiently utilized for various ancillary services such as-energy storage, spinning reserve, voltage stability and frequency regulation.

Thus, with the rapid and parallel developments in the field of SG and EVs, the utilization of EVs for Secondary Frequency Regulation (SFR) would become irresistible. The major pilot projects carried out in [3], [7] further validate the efficacy of V2G mechanism in grid frequency support. Working in this direction, numerous proposals with respect to EV's integration for SFR have been explored in the literature. For example, Peng *et al.* [8] performed a comprehensive review on the different types of the dispatching strategies with respect to SFR using fleet of EVs. According to the authors, these strategies could be broadly classified into two main streams, *i.e.*, *frequency-aware* and *economic-aware*. While, the former deals with maintaining the grid's frequency within the nominals range, the latter deals with the economic benefits linked with the association of V2G services for frequency regulation.

Some of the significant *frequency-aware* dispatch strategies in V2G setup are illustrated as under. In [9], authors explored the concept of EV's participation for SFR using robust optimization framework. However, the major emphasis of the work was on the unidirectional V2G mechanism. In an another work, Kaur *et al.* [1] exploited a colored petri net-based controller for regulating charging and discharging of EVs in accordance with AGC signals. But, the authors confined their work with equal dispatch of regulation signals amongst the Charging Stations (CSs) and Aggregators (AGs). This in turn, leads to either under-utilize or over-utilize the aggregated FRCs of available EVs at CSs. In order to overcome this issue, droop-based optimization strategy was designed by the authors in [10]. Nonetheless, authors neglected battery degradation issues induced due to frequent charging and discharging of EVs' batteries. In the similar context, a comprehensive review of EV's battery degradation for providing effective frequency support services was discussed in [11].

In addition to the above proposals, the *economic-aware* dispatch strategies pertaining to grid frequency support using EVs have been explored in the literature. For instance, authors in [12] used optimization to maximize the benefits of EVs' users while supporting necessary ancillary services. In [6], authors explored the financial benefits of incorporating EVs in the regulation market using stochastic optimization. However, this work neglected the discharging capabilities of EVs and their associated battery deterioration impacts. Working in the similar direction, Yao *et al.* [13] explored the financial benefits of incorporating EVs in the

This article has been accepted for publication in a future issue of this journal, but has not been fully edited. Content may change prior to final publication. Citation information: DOI 10.1109/TSG.2018.2825322, IEEE Transactions on Smart Grid

regulation market. A stochastic optimization problem was formulated by the authors, to estimate the bid of aggregators in the day-ahead market. Nevertheless, EV's discharging needs and the associated battery degradation issues were not explored in this work. Apart from this, authors in [14], [15] used game theoretical models to address energy related issues of data centers using RESs and EVs. Likewise, authors in [16], designed a consolidated energy management system powered with batteries and supported by hybrid Renewable Energy Sources (RESs) using Mixed Integer Linear Programming (MILP). Similarly, MILP was also utilized in [17], wherein energy storage optimization was performed in the grid setup to address the associated economic issues.

MILP is a well researched topic and has been extensively exploited by the researchers to address various issues related to SG. For instance, MILP has been used to model the energy management issues in smart railways powered by photo voltaic generation [18]. On the similar lines, MILP based model has been designed in context of smart houses equipped with RESs, energy storage devices and home appliances [19]. Another MILP-based solution has been proposed in [20], wherein the authors have exploited the advantages of EVs for effective demand response mechanism using Vehicle-to-Home (V2H) and V2G services. MILP-based solutions has also been presented for energy management in Micro Grids (MG). For instance, authors in [21] used mobile and stationary energy storages for efficient energy management in MG setup. MILP has also been utilized in context of university building energy management using charging and discharging characteristics of a fleet of EVs [22].

1.1 Motivation

In view of the above mentioned discussion, it is quite straightforward that EVs would be the most promising demand-side agents for instantaneous SFR in the near future. Nevertheless, it is important to design an highly coordinated, and manageable strategy that can leverage the consolidated participation of EVs for SFR, keeping in view their highly dispersed nature. This concept is best supported through a hierarchical control mechanism relative to a centralized mechanism, which utilizes an array of controllers with fixed functionalities to manage the participation of highly mobile EVs. Additionally, the existing research proposals have focused majorly on unidirectional V2G support rather than bi-directional support. Thus, another significant challenge involves the use V2G mechanism to minimize frequency deviations; while simultaneously sufficing the charging and discharging needs of participating EVs. Above all, a consolidated framework that can reduce EV's battery degradation and maximize their revenue, while they participate in SFR is still missing.

Hence, motivated from these facts, the work presents an integrated solution for effective SFR using fleet of EVs to tackle the above mentioned challenges. To the best of our knowledge, this is the first consolidated framework of its kind, which provides necessary frequency support while handling a varied set of constraints namely-optimal dispatch of AGC signals, minimal battery degradation, maximal bi-directional V2G support and increased participation revenue.

1.2 Contributions

Following contributions are presented in this paper:

- A 2-level hierarchical control scheme is designed in order to demonstrate the benefits of incorporating EVs in centralized mode for instantaneous frequency support.
- An optimal scheduling policy for charging and discharging of EVs using *"Mixed Integer Linear Programming (MILP)"* is designed to minimize the frequency deviations at the grid level while supporting bi-directional V2G capabilities.
- Using the designed MILP based strategy, optimal regulation signal dispatch amongst AGs and CSs is achieved; while reducing EV's battery degradation and increasing their overall revenue for providing ancillary services.
- Finally, the efficacy of the proposed scheme has been demonstrated using real-time traces acquired from *PJM* and *CAISO*.

1.3 Organization

The rest of the article is structured as per the following sequence. The technical description about the proposed 2-level hierarchical control design and the power management scheme has been presented in Section 2 and 3. The details about the regulation traces and experimental results in comparison with an existing technique are given in Section 4. Finally, the article is concluded in Section 5.

2 MILP-based Hierarchical Control Design: System Model

The proposed scheme is a 2-layer hierarchical control scheme having MILP-based optimization. The detailed architectural diagram is depicted in Fig. 1. As evident from the figure, the scheme works at the distribution level wherein fleet of EVs, group of CSs and AGs play a significant role in providing SFR. In the proposed V2G setup, $\mathcal{M}$ number of AGs and $\mathcal{N}$ number of CSs are assumed to be available. These entities along with substation unit (SU) comprise of the physical layer and are assumed to be equipped with the bi-directional and reliable communication links. On the other hand, MILP-based optimizer and FRC estimator deployed at the SU unit, AG and CS levels comprise of the control layer. Due to the presence of these two layers, the proposed scheme is referred as the *2-layer hierarchical control scheme*. At the first level, the proposed framework estimates the regulation signals to be compensated using the joint participation of EVs. Additionally, it also segregates the regulation signal between the AGs and CSs. At the second level, optimal charging and discharging schedules for EVs are determined, while simultaneously minimizing the grid frequency imbalances and maximally satisfying the EVs' power requirements.

The proposed scheme also minimizes the effect of frequent charging and discharging on EV's batteries induced to their participation in the regulation market. This is achieved as follows. SG's frequency index is chosen as an indicator to determine the charging/discharging of EV's batteries; wherein the range of the frequency decides the optimal

This article has been accepted for publication in a future issue of this journal, but has not been fully edited. Content may change prior to final publication. Citation information: DOI 10.1109/TSG.2018.2825322, IEEE Transactions on Smart Grid

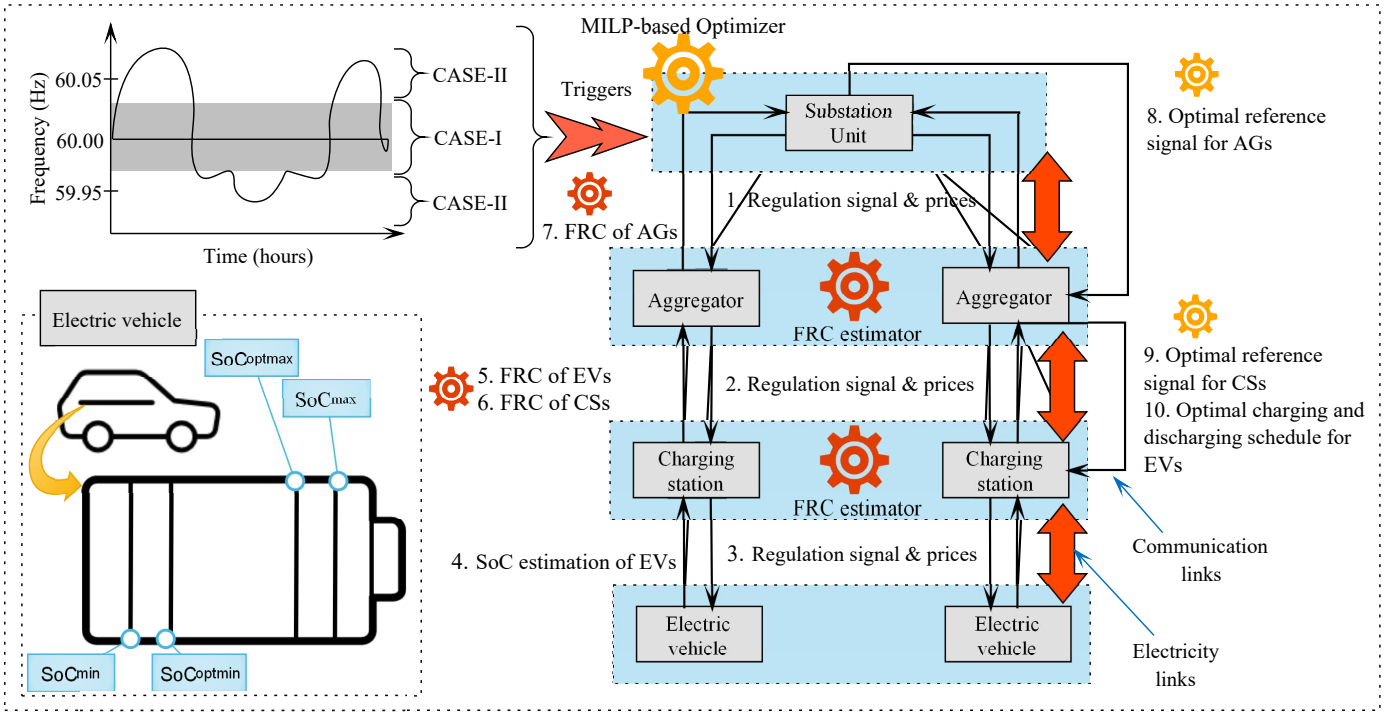

Fig. 1: System model of the proposed MILP-based hierarchical control scheme.

$[SoC_{optmin}, SoC_{optmax}]$ and suboptimal $[SoC_{min}, SoC_{max}]$ State of Charge (SoC) range for EVs' charging and discharging. As depicted in the figure, frequency dead-band used in primary frequency regulation has been taken into account to identify normal (Case-I) and emergency (Case-II) for effective frequency support [23]. In the former case, the SoC range of the EV's battery is kept within the optimal range, while the suboptimal range is used in the latter case. In either case, it is assumed that the decision about charging and discharging of EV's batteries is completely user specific. Additionally, EVs' users participate in the secondary regulation process in order to earn higher rewards. Hence, SoC of the EVs when they are to be used by their respective owners is either maintained between the optimal SoC range or the suboptimal range.

The working philosophy of the scheme is diagrammatically shown using Fig. 1. Here, SU is used for monitoring frequency fluctuations and relaying the real-time regulation signals ($\mathfrak{R}^{ref}(t)$). Also, the SU relays regulation up and down prices at time t ($\mathfrak{Pr}^{up}(t)$ & $\mathfrak{Pr}^{down}(t)$). In response to these signals, FRC estimators (deployed at AG and CS levels) compute the FRCs of the participating EVs, CSs and AGs. Using this information, MILP-based optimizer at SU level generates an optimal schedule for charging and discharging EVs across the time horizon (T), to track the regulation signal. This is done while simultaneously minimizing battery degradation and maximizing EV's revenue in the entire process. Additionally, MILP-based optimizer also dispatches the regulation signal amongst the AGs and CSs in an optimal manner.

In order to support real time SG operations, the underlying communication channel in SG should be capable of low latency along with improved capacity, coverage and high data rate. This is in accordance with the latest guidelines released by NIST [24]. With this, the communication technologies in SG domain has witnessed a major blow in the last couple of years; ranging from Power Line Communication, IEEE 802.15.4 (ZigBee), IEEE 802.11 (Wireless LAN), IEEE 802.16 (WiMAX), GSM, and GPRS to Optical Fiber and LTE/LTE-A. However, the most sought after wireless technology is this regard is 3GPP Long Term Evolution (LTE) Release 8 [25]. One of the distinctive advantages of LTE is its ability to schedule resources in both Time Domain Duplex (TDD) and Frequency Domain Duplex (FDD) modes. Hence, the communication links from the higher levels to lower ones in the considered hierarchical setup are assumed to be supported by the robust LTE, in view of minimal communication delay. However, in case of possible disturbances (like link failures), the proposed scheme adopts a fault tolerant mechanism as detailed in Algorithm 1. Nevertheless, the proposed mechanism does not provided exact frequency support but is capable of providing acceptable frequency support during communication breakdowns.

Algorithm 1 Coordinated grid frequency support during communication disturbances.

Input: $\mathfrak{R}_{ij}^{ref}(t)$, $\mathfrak{R}_{ij}^{ref}(t-1)$, t, and $t-1$

1: **if** (Communication between i^{th} AG and j^{th} CS collapses) **then**
2: Set $\mathfrak{R}_{ij}^{ref}(t) = \mathfrak{R}_{ij}^{ref}(t-1)$ from time stamp $(t-1)$
3: **end if**

The working of the algorithm can be understood as follows. Say the communication channel between the i^{th} AG and j^{th} CS collapses at time stamp t; due to which the latest regulation signal ($\mathfrak{R}_{ij}^{ref}(t)$) could not be communicated. Under such scenarios, the affected CS, *i.e.*, j^{th} CS continues

This article has been accepted for publication in a future issue of this journal, but has not been fully edited. Content may change prior to final publication. Citation information: DOI 10.1109/TSG.2018.2825322, IEEE Transactions on Smart Grid

to operates with the previously relayed regulation signal ($\mathfrak{R}_{ij}^{ref}(t-1)$) at time stamp $t-1$.

3 Problem Formulation

The problem is formulated as follows:

1) min $\mathbb{F}(C_{ij}^{sch}(t), D_{ij}^{sch}(t)) = \mathbb{F}_1 - \mathbb{F}_2 - \mathbb{F}_3 + \mathbb{F}_4 - \mathbb{F}_5$ *subject to:*
2) total FRC constraint Eqs. (10)-(18)
3) battery constraints Eqs. (19)-(21)
4) reference signal dispatch constraint Eq. (5)
5) $C_{ij}^{sch}(t) \geq 0; \forall i, j$
6) $D_{ij}^{sch}(t) \geq 0; \forall i, j$
7) $C_{ijk}^{sch}(t) \geq 0; \forall i, j, k$
8) $D_{ijk}^{sch}(t) \geq 0; \forall i, j, k$

The above defined problem takes into account multiple objectives such as-minimization of frequency deviations ($\mathbb{F}_1$), maximal V2G support ($\mathbb{F}_2$ and $\mathbb{F}_3$), optimal dispatch of reference signals ($\mathbb{F}_4$) and EV's revenue maximization ($\mathbb{F}_5$). The constraints taken into consideration impose restrictions on EV's battery charging and discharging processes to prevent battery degradation. Along with this, FRCs of EVs, CSs and AGs are also kept in check so as to provide reliable frequency support and ensure optimal dispatch of reference signals accordingly. It is worth mentioning here, that the proposed work considers equal weights for all the objective functions, since these weights depict the relative importance of an objective function over another in the given context. The concept has been adopted in order to compute the optimal solution without prioritizing any function over the other [26], [27], [28], [29].

The problem formulated above is '*Mixed Integer Linear Programming Problem*', wherein $C_{ij}^{sch}(t)$ and $D_{ij}^{sch}(t)$ are the decision variables. These variables denote the scheduled charging and discharging rates of the EV under consideration. The defined problem is solved using the Mosek solver [30].

3.1 List of Objective Functions

3.1.1 Minimization of Frequency Deviations

Function ($\mathbb{F}_1(C_{ij}^{sch}(t), D_{ij}^{sch}(t))$) deals with the minimization of frequency deviations wherein the cumulative FRCs of EVs is used to track the $\mathfrak{R}^{ref}(t)$ across all time stamps t. This is mathematically expressed as follows.

$$\begin{aligned}\min\ \mathbb{F}_1(C_{ij}^{sch}(t), D_{ij}^{sch}(t)) = \\ \Big(\mathfrak{R}^{ref}(t) - \sum_{i\in\mathcal{M}}\sum_{j\in\mathcal{N}}\Big(\sum_{k\in k_j}\frac{-SoC_{ijk}^{c}(t)\times E_{ijk}^{rated}}{100}\Big)\times C_{ij}^{sch}(t) \\ + \sum_{i\in\mathcal{M}}\sum_{j\in\mathcal{N}}\Big(\sum_{k\in k_j}\frac{SoC_{ijk}^{d}(t)\times E_{ijk}^{rated}}{100}\Big)\times D_{ij}^{sch}(t)\Big)\end{aligned} \tag{1}$$

In the above equations, $SoC_{ijk}^{c}(t)$ is equivalent to either $(SoC_{optmax} - SoC_{ijk}^{c,ini}(t))$ or $(SoC_{max} - SoC_{ijk}^{c,ini}(t))$ as per C-I or C-II respectively. Similarly, $SoC_{ijk}^{d}(t)$ is defined such that $C_{ij}^{sch}(t)$ and $D_{ij}^{sch}(t)$ depict the scheduled charging and discharging rates for EVs available at the j^{th} CS of i^{th} AG.

3.1.2 Maximal V2G Support

Another important contribution of the present manuscript is to provide maximal V2G support for simultaneous charging and discharging of EVs. This is achieved using the below mentioned functions namely-$\mathbb{F}_2(C_{ij}^{sch}(t), 0)$ and $\mathbb{F}_3(0, D_{ij}^{sch}(t))$ respectively.

$$\begin{aligned}\max\ \mathbb{F}_2(C_{ij}^{sch}(t), 0) = \\ \Big(\sum_{i\in\mathcal{M}}\sum_{j\in\mathcal{N}}\Big(\sum_{k\in k_j}\frac{-SoC_{ijk}^{c}(t)\times E_{ijk}^{rated}}{100}\Big)\times C_{ij}^{sch}(t)\Big)\end{aligned} \tag{2}$$

$$\begin{aligned}\max\ \mathbb{F}_3(0, D_{ij}^{sch}(t)) = \\ \Big(\sum_{i\in\mathcal{M}}\sum_{j\in\mathcal{N}}\Big(\sum_{k\in k_j}\frac{SoC_{ijk}^{d}(t)\times E_{ijk}^{rated}}{100}\Big)\times D_{ij}^{sch}(t)\Big)\end{aligned} \tag{3}$$

3.1.3 Optimal Reference Signal Dispatch amongst CSs and AGs

As mentioned in the previous section, optimal reference signal dispatch amongst the CSs ($\mathfrak{R}_{ij}^{ref,sch}(t)$) and AGs ($\mathfrak{R}_{i}^{ref,sch}(t)$) is also an important consideration for achieving reliable frequency support using fleet of EVs. This is particularly important so that maximum available FRCs of the CSs and AGs could be exploited in the best possible manner. Additionally, it also ensures that none of the AGs and CSs are left under-utilized or over-utilized by randomly dispatching them reference signals. Here, negative reference signals depict regulation down signals, while positive reference signals represent regulation up signals. The computation of $\mathfrak{R}_{ij}^{ref,sch}(t)$ is done as per the below mentioned function, *i.e.*, $\mathbb{F}_4(C_{ij}^{sch}(t), D_{ij}^{sch}(t))$.

$$\begin{aligned}\min\ \mathbb{F}_4(C_{ijk}^{sch}(t), D_{ijk}^{sch}(t)) = \\ \Big(\mathfrak{R}^{ref}(t) - \sum_{i\in\mathcal{M}}\sum_{j\in\mathcal{N}}\{\mathfrak{R}_{11}^{ref,sch}(t) + ... + \mathfrak{R}_{mn}^{ref,sch}(t)\}\Big)\end{aligned} \tag{4}$$

where,

$$\begin{aligned}\mathfrak{R}_{ij}^{ref,sch}(t) = \\ \begin{cases}\mathfrak{R}^{ref}(t)\times\dfrac{\mathfrak{F}_{ij}^{up}(t)}{\sum_{i\in\mathcal{M}}\sum_{j\in\mathcal{N}}\mathfrak{F}_{ij}^{up}(t)}; \text{if } \mathfrak{R}^{ref}(t)\geq 0 \\ \mathfrak{R}^{ref}(t)\times\dfrac{\mathfrak{F}_{ij}^{down}(t)}{\sum_{i\in\mathcal{M}}\sum_{j\in\mathcal{N}}\mathfrak{F}_{ij}^{down}(t)}; \text{if } \mathfrak{R}^{ref}(t)< 0\end{cases}\end{aligned} \tag{5}$$

Moreover, the computation of reference signals for the individual AGs ($\mathfrak{R}_{i}^{ref,sch}(t)$) is done as follows.

$$\mathfrak{R}_{i}^{ref,sch}(t) = \sum_{j=1}^{\mathcal{N}}\mathfrak{R}_{ij}^{ref,sch}(t);\ \forall i \tag{6}$$

3.1.4 Revenue Maximization of EVs for SFR

EV's which participate in ancillary market are also provided incentives from ISO. Generally, this payment is made $\$/MW$ and it varies for both the regulation up ($\mathfrak{Pr}^{up}(t)$) and down ($\mathfrak{Pr}^{down}(t)$) services. Hence, the cumulative revenue earned by the fleet of EVs in a particular time interval (t) is formulated using the below mentioned function ($\mathbb{F}_5(C_{ij}^{sch}(t), D_{ij}^{sch}(t))$).

This article has been accepted for publication in a future issue of this journal, but has not been fully edited. Content may change prior to final publication. Citation information: DOI 10.1109/TSG.2018.2825322, IEEE Transactions on Smart Grid

$$\max\ \mathbb{F}_5(C_{ij}^{sch}(t), D_{ij}^{sch}(t)) = \sum_{i\in\mathcal{M}}\sum_{j\in\mathcal{N}}\sum_{k\in k_j}\Big((\mathfrak{F}_{ijk}^{up}(t)\times\mathfrak{Pr}^{up}(t)) + (\mathfrak{F}_{ijk}^{down}(t)\times\mathfrak{Pr}^{down}(t)\Big) \quad (7)$$

In detail, the above equation can be represented as follows:

For Case-I:

$$\begin{aligned}\max\ \mathbb{F}_5(C_{ij}^{sch}(t), D_{ij}^{sch}(t)) = \sum_{i\in\mathcal{M}}\sum_{j\in\mathcal{N}}\sum_{k\in k_j}\\ \Big(\Big(\Big(SoC_{ijk}^{d,ini}(t) - SoC_{optmin}\Big)\times\frac{E_{ijk}^{rated}\times D_{ijk}^{sch}(t)}{100}\\ \times\mathfrak{Pr}^{up}(t)\Big)+\\ \Big(-\Big(SoC_{optmax} - SoC_{ijk}^{c,ini}(t)\Big)\times\frac{E_{ijk}^{rated}\times C_{ijk}^{sch}(t)}{100}\\ \times\mathfrak{Pr}^{down}(t)\Big)\Big)\end{aligned} \quad (8)$$

For Case-II:

$$\begin{aligned}\max\ \mathbb{F}_5(C_{ij}^{sch}(t), D_{ij}^{sch}(t)) = \sum_{i\in\mathcal{M}}\sum_{j\in\mathcal{N}}\sum_{k\in k_j}\\ \Big(\Big(\Big(SoC_{ijk}^{d,ini}(t) - SoC_{min}\Big)\times\frac{E_{ijk}^{rated}\times D_{ijk}^{sch}(t)}{100}\\ \times\mathfrak{Pr}^{up}(t)\Big)+\\ \Big(-\Big(SoC_{max} - SoC_{ijk}^{c,ini}(t)\Big)\times\frac{E_{ijk}^{rated}\times C_{ijk}^{sch}(t)}{100}\\ \times\mathfrak{Pr}^{down}(t)\Big)\Big)\end{aligned} \quad (9)$$

The detailed explanation with respect to $\mathfrak{F}_{ijk}^{up}(t)$ and $\mathfrak{F}_{ijk}^{down}(t)$ is provided in the upcoming segment.

3.2 List of Constraints

3.2.1 Estimation of FRCs of EVs, CSs and AGs

The available FRC of EVs is calculated in response of the regulation up and down signals. Hence, EV's FRCs is symbolically represented using two symbols, *i.e.*, $\mathfrak{F}_{ijk}^{up}(t)$ and $\mathfrak{F}_{ijk}^{down}(t)$. Here, $\mathfrak{F}_{ijk}^{up}(t)$ denotes the FRC of the i^{th} EV for providing regulation up services, whereas the parameter $\mathfrak{F}_{ijk}^{down}(t)$ represents the FRC of the EV for sustaining regulation down services at t instant. The mathematically representation for the same is illustrated as follows:

$$\mathfrak{F}_{ijk}^{up}(t) = \begin{cases}\Big(SoC_{ijk}^{d,ini}(t) - SoC_{optmin}\Big)\times\dfrac{E_{ijk}^{rated}\times D_{ijk}^{sch}(t)}{100}; \textit{C-I}\\ \Big(SoC_{ijk}^{d,ini}(t) - SoC_{min}\Big)\times\dfrac{E_{ijk}^{rated}\times D_{ijk}^{sch}(t)}{100}; \textit{C-II}\end{cases} \quad (10)$$

$$\mathfrak{F}_{ijk}^{down}(t) = \begin{cases}-\Big(SoC_{optmax} - SoC_{ijk}^{c,ini}(t)\Big)\times\dfrac{E_{ijk}^{rated}\times C_{ijk}^{sch}(t)}{100}; \textit{C-I}\\ -\Big(SoC_{max} - SoC_{ijk}^{c,ini}(t)\Big)\times\dfrac{E_{ijk}^{rated}\times C_{ijk}^{sch}(t)}{100}; \textit{C-II}\end{cases} \quad (11)$$

In the above equations, the indices i and j denote the respective AG and CS under consideration. The initial SoC of k^{th} EV seeking charging/discharging at time t is represented using $SoC_{ijk}^{c,ini}(t)/SoC_{ijk}^{d,ini}(t)$. EV's scheduled charging and discharging rates are denoted using $C_{ijk}^{sch}(t)$ and $D_{ijk}^{sch}(t)$ respectively. Moreover, values of $\mathfrak{F}_{ijk}^{up}(t)$ and $\mathfrak{F}_{ijk}^{down}(t)$ are computed in accordance with the categorization of frequency deviations into Case-I (*C-I*) and II (*C-II*) respectively. These computed FRC values ($\mathfrak{F}_{ijk}^{up}(t)$ and $\mathfrak{F}_{ijk}^{down}(t)$) are nothing but the amounts of the power that are either dispatched from the vehicles to grid (*i.e.*, V2G) or withdrawn by the vehicle from the grid (*i.e.*, Grid-to-Vehicle). Additionally, EV's charging/discharging time would be proportional to its corresponding FRC. In other words, it is considered as a function of EV's initial SoC level ($SoC_{ijk}^{d,ini}(t)$ and $SoC_{ijk}^{c,ini}(t)$), E_{ijk}^{rated}, $C_{ijk}^{sch}(t)$ and $D_{ijk}^{sch}(t)$.

It is worth mentioning here that the above mentioned approach helps to keep the final SoC level of EV's battery either in the optimal or the suboptimal SoC range. Nevertheless, the proposed scheme can also be extended to the case; wherein user's specify the EV's final SoC range. This can be achieved by remodeling Eqs. (10) and (11) with the following equations respectively.

$$\mathfrak{F}_{ijk}^{up}(t) = \Big(SoC_{ijk}^{d,ini}(t) - SoC_{min}^{usr}\Big)\times\frac{E_{ijk}^{rated}\times D_{ijk}^{sch}(t)}{100} \quad (12)$$

$$\mathfrak{F}_{ijk}^{down}(t) = -\Big(SoC_{max}^{usr} - SoC_{ijk}^{c,ini}(t)\Big)\times\frac{E_{ijk}^{rated}\times C_{ijk}^{sch}(t)}{100} \quad (13)$$

In the above equations, the FRCs of the participating EVs is computed in accordance with the user specified SoC ranges for charging (SoC_{max}^{usr}) and discharging (SoC_{min}^{usr}) respectively. However, such an approach may undermine the relative importance of the proposed scheme for minimizing battery degradation.

Using the above equations, the FRCs of CSs ($\mathfrak{F}_{ij}^{up}(t)$ and $\mathfrak{F}_{ij}^{down}(t)$) and AGs ($\mathfrak{F}_{i}^{up}(t)$ and $\mathfrak{F}_{i}^{down}(t)$) for regulation up and down services is computed using the following set of equations.

$$\mathfrak{F}_{ij}^{up}(t) = \sum_{j\in\mathcal{N}}\sum_{k\in k_j}\mathfrak{F}_{ijk}^{up}(t) \quad (14)$$

$$\mathfrak{F}_{ij}^{down}(t) = \sum_{j\in\mathcal{N}}\sum_{k\in k_j}\mathfrak{F}_{ijk}^{down}(t) \quad (15)$$

$$\mathfrak{F}_{i}^{up}(t) = \sum_{i\in\mathcal{M}}\sum_{j\in\mathcal{N}}\sum_{k\in k_j}\mathfrak{F}_{ijk}^{up}(t) \quad (16)$$

$$\mathfrak{F}_{i}^{down}(t) = \sum_{i\in\mathcal{M}}\sum_{j\in\mathcal{N}}\sum_{k\in k_j}\mathfrak{F}_{ijk}^{down}(t) \quad (17)$$

3.2.2 Total FRC Constraint

The total FRC ($\mathfrak{F}^{tot}(t)$) of the considered V2G setup is computed using the following equation, wherein $\mathfrak{F}^{tot}(t)$ is defined as the sum of the total FRCs of the participating EVs supporting both regulation up and down services.

$$\mathfrak{F}^{tot}(t) = \sum_{i\in\mathcal{N}}\mathfrak{F}^{up}(t) + \sum_{i\in\mathcal{N}}\mathfrak{F}^{down}(t) \quad (18)$$

This article has been accepted for publication in a future issue of this journal, but has not been fully edited. Content may change prior to final publication. Citation information: DOI 10.1109/TSG.2018.2825322, IEEE Transactions on Smart Grid

3.2.3 EV's Battery Charging & Discharging Constraint

Studies suggest that maintaining the SoC level of the EV's batteries in a reasonable range plays a significant role in maximizing the battery's lifetime. Existing research studies suggest to maintain SoC levels with the permissible range of $[SoC_{max}, SoC_{min}]$. Here, parameters SoC_{max} and SoC_{min} denote the minimum and maximum SoC levels up to which the EV's batteries should be charged and discharged respectively [1], [10]. However, recent experimental validation done by National Renewable Energy Laboratory on Li-ion batteries has lead to contrasting results [23]. The obtained results indicate that the batteries which maintain their SoC levels in the range of 30-50% (throughout their life time) have comparatively slower battery degradation rates than the batteries which maintain their SoC in the ranges of 70-90% and 20%-40%. Hence, motivated by this fact, authors in [23] have used the battery characteristics as depicted in Fig. 1. As indicated in the figure, EV's batteries can have different SoC level namely-SoC_{max}, SoC_{optmax}, SoC_{optmin} and SoC_{min}. EV's batteries in the proposed frequency support setup are categorized to provide SFR support under varied circumstances. For instance, during normal circumstances (C-I) EV's maintain their current SoC levels ($SoC^{cur}_{ijk}(t)$) in an optimal range of $SoC_{optmin} \leq SoC^{cur}_{ijk}(t) \leq SoC_{optmax}$. On the other hand, EVs tend to provide enhanced FRCs by pushing their SoC levels in the suboptimal range $SoC_{min} \leq SoC^{cur}_{ijk}(t) \leq SoC_{max}$ under C-II. This is represented as follows.

$$SoC^{cur}_{ijk}(t) = \begin{cases} SoC_{optmin} \leq SoC^{cur}_{ijk}(t) \leq SoC_{optmax}; \textit{C-I} \\ SoC_{min} \leq SoC^{cur}_{ijk}(t) \leq SoC_{max}; \textit{C-II} \end{cases} \tag{19}$$

Apart from maintaining the SoC levels of the EV's batteries within the optimal range, the present work also extends the concept of maintaining $C^{sch}_{ijk}(t)$ and $D^{sch}_{ijk}(t)$ in the optimal and sub-optimal ranges. It is mathematically represented as follows:

$$C^{sch}_{ijk}(t) = \begin{cases} C_{optmin} \leq C^{sch}_{ijk}(t) \leq C_{optmax}; \textit{C-I} \\ C_{min} \leq C^{sch}_{ijk}(t) \leq C_{max}; \textit{C-II} \end{cases} \tag{20}$$

$$D^{sch}_{ijk}(t) = \begin{cases} D_{optmin} \leq D^{sch}_{ijk}(t) \leq D_{optmax}; \textit{C-I} \\ D_{min} \leq D^{sch}_{ijk}(t) \leq D_{max}; \textit{C-II} \end{cases} \tag{21}$$

4 Results and Discussions

This section presents in detail the simulation strategy considered for the evaluation of the proposed scheme on real-time traces acquired from PJM [31] and CAISO [32]. The results have been evaluated using Mosek solver [30]. Additionally, it also highlights the comparison of the proposed scheme against the existing technique [10].

The considered simulation setup takes into account the parameters illustrated in Table-1 for evaluating the proposed scheme on 24 hours timescale. As evident from the table, the case-study comprises of 3 AGs (AG_1, AG_2, AG_3) and 6 CSs ($CS_{11}, CS_{12}, CS_{21}, CS_{22}, CS_{23}, CS_{31}$) in total for providing effective grid ancillary services using fleet of EVs. However, the proposed scheme is extensible for $\mathcal{M}$ number of AGs and $\mathcal{N}$ of CSs.

The real-time traces have been acquired from PJM and CAISO for performing extensive simulations. Data from the two sources corresponds to the real-time regulation signals and prices for providing reliable regulation up and down services respectively. These data sets have depicted using Figs. 2a and 2b. For instance, at 2000 hours $\mathfrak{R}^{ref}(t)$ of -176.88 kW was triggered due to demand and supply imbalances. The corresponding regulation prices offered by the ISO to manage the frequency deviations were 5.5 \$/kW and 3.5 \$/kW respectively for regulation up and down services. These deviations in grid's frequency is depicted using Fig. 2c. At 2000 hours, frequency deviations of -0.01 Hz (C-I) was observed due to demand and supply imbalances. The total number of the EVs considered in the simulation setup is shown using Fig. 2d, wherein 179 and 180 EVs at the CSs were participated in charging and discharging activities respectively. The rebalancing of these fluctuations is catered as follows.

TABLE 1: Simulation parameters considered

Parameters	Values	Parameters	Values
No. of AGs	3	Case-I:$\lvert\Delta f\rvert$	≤ 0.2
No. of CSs	6	Case-II:$\lvert\Delta f\rvert$	≥ 0.2
No. of EVs/CS	0-60	E^{rated}_{ijk}	16
SoC_{optmax}	70	C_{optmax}/D_{optmax}	1.5
SoC_{max}	90	C_{max}/D_{max}	2
SoC_{optmin}	40	C_{optmin}/D_{optmin}	0.5
SoC_{min}	20	C_{min}/D_{min}	0

The FRC estimator computed the cumulative FRCs of the AGs, *i.e.*, $\mathfrak{F}^{up}_i(t)$ and $\mathfrak{F}^{down}_i(t)$. The estimated values across 24 hours are shown using Fig. 2e. For instance, at 2000 hours $\mathfrak{F}^{up}_i(t)$ and $\mathfrak{F}^{down}_i(t)$ values were found to be 412.6 and -830.4 kW respectively. Based on these values, the regulation signal of -176.88 kW was dispatched amongst the AGs and CSs using the designed MILP-based problem. The reference signals segregated amongst the AGs and CSs are highlighted in Figs. 2f and 2g. At 2000 hours, the scheduled reference signals for the CSs were found to be -40.61, -22.70, -25.94, -47.75, -15.71, and -24.14 kW respectively. This segregation of $\mathfrak{R}^{ref}(t)$ is in accordance with the respective FRCs of the CSs. This is done so as to achieve the full capacity of the underlying CSs for providing effective and reliable frequency support. In order to reflect the same, the concept of optimal and maximum/minimum charging/discharging has been introduced in Section 3.2.3. The related results have been pictorially represented using Figs. 2h and 2i respectively. For instance, at 2000 hours, the $C^{sch}_{ij}(t)$ and $D^{sch}_{ij}(t)$ varied between the optimal range as the frequency deviations were classified as C-I. Thereby, reducing the battery degradation impacts on the EVs' batteries.

Due to the alteration in $C^{sch}_{ij}(t)$ and $D^{sch}_{ij}(t)$ values, significant change in the SoC levels of the participating EVs was observed. The corresponding results have been represented using Fig. 2j. The figure clearly depicts the average SoC variations of the EVs' batteries over the regulation process; wherein, the SoC levels of the batteries were always maintained within the optimal range; hence, minimizing the impact of battery degradation. In addition to this, the results also indicate the proposed scheme caters the charging and discharging requirements of the EVs across all the CSs.

In addition to the above mentioned contributions, the proposed scheme also aims to maximize EVs' profit margins by involving them in different time slots as per $\mathfrak{Pr}^{up}(t)$ and $\mathfrak{Pr}^{down}(t)$ values. Hence, the corresponding findings to maximize EV's revenue are summarized in Fig. 2k. As de-

This article has been accepted for publication in a future issue of this journal, but has not been fully edited. Content may change prior to final publication. Citation information: DOI 10.1109/TSG.2018.2825322, IEEE Transactions on Smart Grid

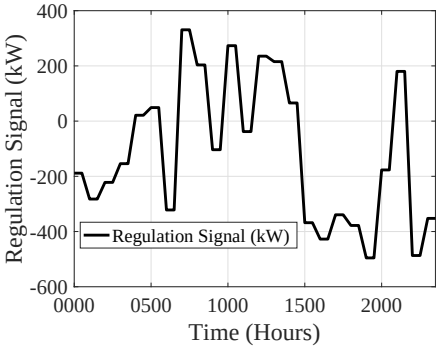

(a) PJM regulation signals with respect to 6^{th} June 2014.

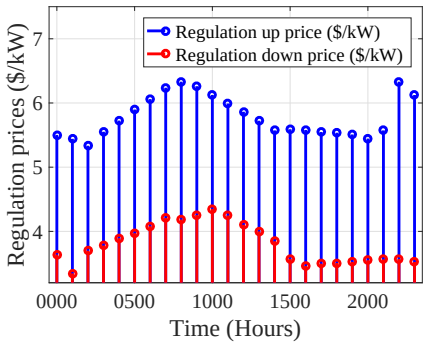

(b) Regulation up and down prices acquired from CAISO for the year 2014.

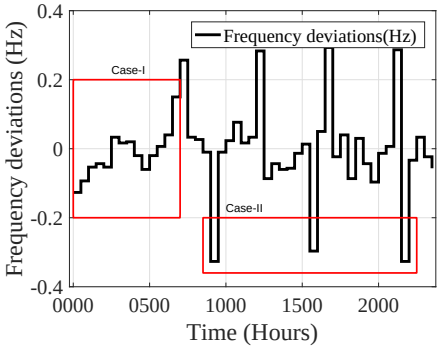

(c) Grid frequency fluctuations.

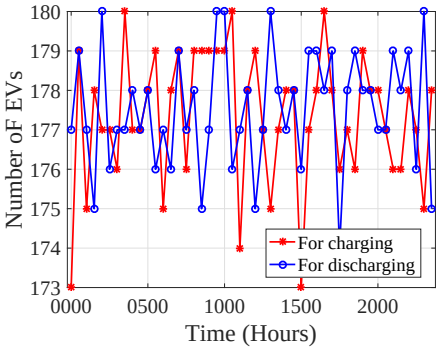

(d) Total number of EVs for charging and discharging

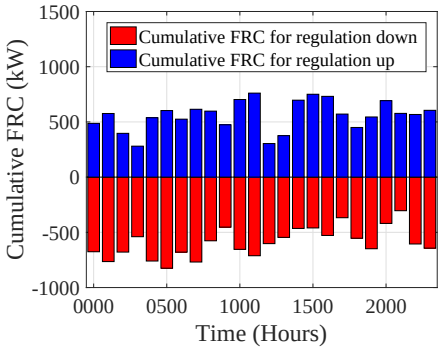

(e) Cumulative FRCs for regulation up and down services.

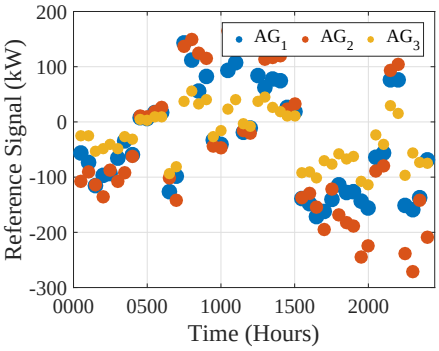

(f) Dispatch of regulation signals across aggregators.

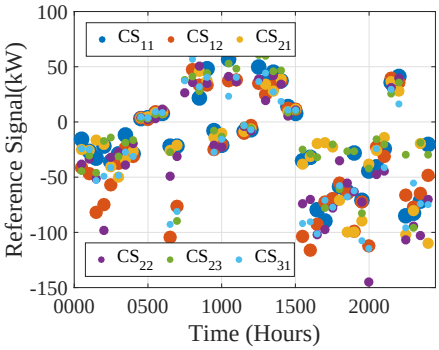

(g) Dispatch of regulation signals across charging stations.

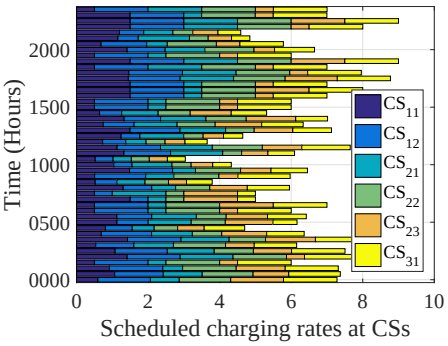

(h) Scheduled $C_{ij}^{sch}(t)$ of participating EVs at different CSs.

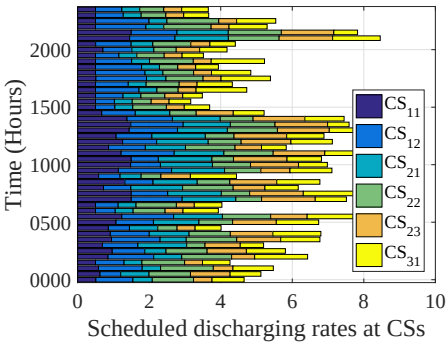

(i) Scheduled $D_{ij}^{sch}(t)$ of participating EVs at different CSs.

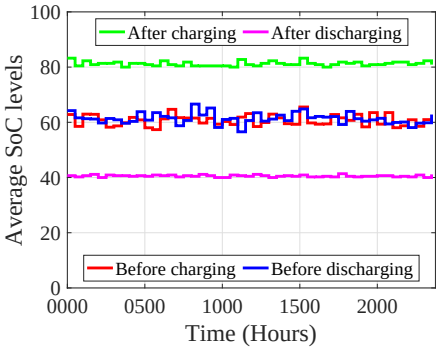

(j) Average SoC variations before and after charging and discharging activities.

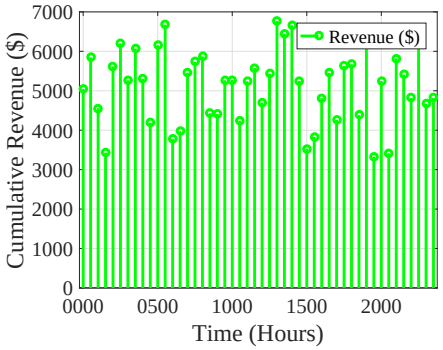

(k) Cumulative revenue earned by the EVs available at different CSs.

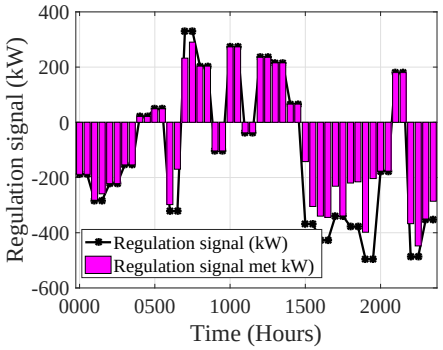

(l) Regulation support using the proposed scheme.

Fig. 2: Performance results obtained using the proposed scheme.

This article has been accepted for publication in a future issue of this journal, but has not been fully edited. Content may change prior to final publication. Citation information: DOI 10.1109/TSG.2018.2825322, IEEE Transactions on Smart Grid

picted in the figure, the cumulative revenue earned by EVs across all the CSs at 2000 hours was found to approximately $5245.7.

Finally, the primary agenda of the proposed scheme was to minimize the frequency fluctuations using integrated fleet of EVs. Hence, the regulation power met using the proposed scheme is highlighted using Fig. 2l. The results clearly depict the proposed scheme tracks the regulation signal in majority of the cases *e.g.* at 2000 hours.

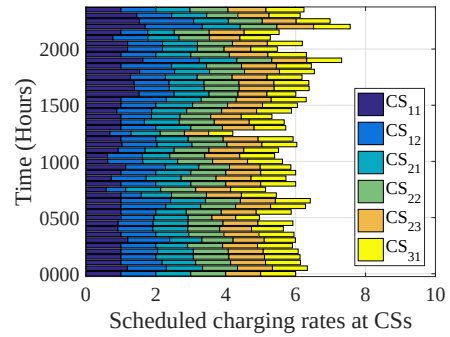

(a) Scheduled $C_{ij}^{sch}(t)$ using the existing scheme.

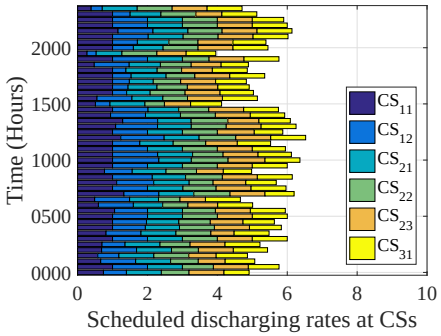

(b) Scheduled $D_{ij}^{sch}(t)$ using the existing scheme.

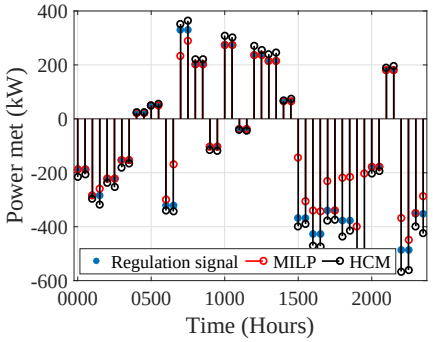

(c) Regulation support using the proposed scheme and the existing scheme.

Fig. 3: Comparison of the proposed scheme and the existing scheme [10].

4.1 Comparison with an existing scheme

To evaluate the efficacy of the proposed scheme, an existing scheme presented in [10] has been taken into account. It has the maximum resemblance to the proposed technique except the consideration of EV's revenue and their battery degradation. Hence, it has been chosen for evaluating the efficacy of the proposed scheme.

For the sake of clarity, the datasets as shown in Figs. 2a and 2b along with the parameters highlighted in Table-1 have been considered for performing the comparative evaluation of the two schemes. The results obtained are highlighted using Fig. 2. The considered existing scheme is ideally a 2-layer hierarchical control scheme (HCM) based on droop mechanism using which it segregates the reference signals amongst the CSs and AGs. On the other hand, the proposed scheme is based on the robust MILP-based optimization techniques which dispatches the reference signals according the FRCs of the participating AGs and CSs. Additionally, the computation of $C_{ijk}^{sch}(t)$ and $D_{ijk}^{sch}(t)$ is also widely apart. Due to these reasons, the two schemes defer in achieving reliable frequency support as shown in Fig. 3c. It is evident from the results that the proposed scheme achieves superior results than the existing scheme in terms of tracking the regulation signal.

Moreover, the relative comparison of the two schemes in terms of regulating the $C_{ijk}^{sch}(t)$ and $D_{ijk}^{sch}(t)$ is shown using Figs. 2h and 3a, and Figs. 2i and 3b. The results clearly depict the existing scheme fails to maintain the $C_{ijk}^{sch}(t)$ and $D_{ijk}^{sch}(t)$ within the optimal limits even during normal scenario (C-I), leading to higher battery degradation issues. On the other hand, the proposed scheme tracks the regulation signal much more efficiently while keeping the $C_{ijk}^{sch}(t)$ and $D_{ijk}^{sch}(t)$ within the optimal range. Thus, the results clearly validate the efficacy of the proposed scheme in terms of its implementation in real-time scenario.

5 Conclusion and Future Remarks

The work presented a *"MILP-based Hierarchical Control Design"* for secondary frequency regulation (SFR) using integrated fleet of electric vehicles (EVs). The proposed work explored the potential of incorporating EVs in SFR in a centralized mode wherein primary focus was to minimize grid frequency deviations. Moreover, the proposed work also concentrated on maximal V2G support, optimal dispatch of reference signals, reduced battery degradation and increased incentives to EVs for participating in the regulation market. This complex problem was addressed by formulating using *'Mixed Integer linear programming (MILP)'* which in-turn formed the control layer of the proposed hierarchical control scheme. The proposed work has been experimentally validated to real-time traces acquired from *PJM* and *CAISO*. Also, the proposed scheme has been compared with an existing scheme and the obtained results indicate superior performance of the proposed scheme.

In the future, we would like to extend this work to distributed control of EVs for effective SFR.

Acknowledgment

This work is supported by fellowship sponsored by the Tata Consultancy Services (TCS), India.

References

[1] K. Kaur, R. Rana, N. Kumar, M. Singh, and S. Mishra, "A Colored Petri Net Based Frequency Support Scheme Using Fleet of Electric Vehicles in Smart Grid Environment," *IEEE Transactions on Power Systems*, vol. 31, no. 6, pp. 4638–4649, 2016.

[2] T. Masuta and A. Yokoyama, "Supplementary load frequency control by use of a number of both electric vehicles and heat pump water heaters," *IEEE Transactions on Smart Grid*, vol. 3, no. 3, pp. 1253–1262, 2012.

[3] W. Kempton, V. Udo, K. Huber, K. Komara, S. Letendre, S. Baker, D. Brunner, and N. Pearre, "A test of vehicle-to-grid (V2G) for energy storage and frequency regulation in the PJM system," *Results from an Industry-University Research Partnership*, vol. 32, 2008.

[4] K. Kaur, M. Singh, and N. Kumar, "Multi-objective Optimization for Frequency Support using Electric Vehicles: An Aggregator-based Hierarchical Control Mechanism," *IEEE Systems Journal*, 2017, doi: 10.1109/JSYST.2017.2771948.

[5] Global EV outlook 2016 Beyond one million electric cars. International Energy Agency. [Accessed on: Apr 2017]. [Online]. Available: https://www.iea.org/publications/freepublications/publication/Global_EV_Outlook_2016.pdf

[6] W. Kempton and J. Tomić, "Vehicle-to-grid power implementation: From stabilizing the grid to supporting large-scale renewable energy," *Journal of power sources*, vol. 144, no. 1, pp. 280–294, 2005.

[7] H. Ni, "PJM advanced technology pilots for system frequency control," in *2012 IEEE PES Innovative Smart Grid Technologies (ISGT)*, 2012, pp. 1–6.

[8] C. Peng, J. Zou, and L. Lian, "Dispatching strategies of electric vehicles participating in frequency regulation on power grid: A review," *Renewable and Sustainable Energy Reviews*, vol. 68, pp. 147–152, 2017.

[9] E. Yao, V. W. Wong, and R. Schober, "Robust frequency regulation capacity scheduling algorithm for electric vehicles," *IEEE Transactions on Smart Grid*, vol. 8, no. 2, pp. 984–997, 2017.

[10] K. Kaur, M. Singh, and N. Kumar, "Fleet of electric vehicles for frequency support in Smart Grid using 2-layer hierarchical control mechanism," in *2016 IEEE Power and Energy Society General Meeting (PESGM)*, 2016, pp. 1–5.

[11] S. Han, S. Han, and H. Aki, "A practical battery wear model for electric vehicle charging applications," *Applied Energy*, vol. 113, pp. 1100–1108, 2014.

[12] S. Han and S. Han, "Economic feasibility of V2G frequency regulation in consideration of battery wear," *Energies*, vol. 6, no. 2, pp. 748–765, 2013.

[13] E. Yao, V. W. Wong, and R. Schober, "Optimization of Aggregate Capacity of PEVs for Frequency Regulation Service in Day-Ahead Market," *IEEE Transactions on Smart Grid*, 2016, doi: 10.1109/TSG.2016.2633873.

[14] G. S. Aujla, R. Chaudhary, N. Kumar, J. Rodrigues, and A. Vinel, "SDN-Based Data Center Energy Management System Using RES and Electric Vehicles," in *2016 IEEE Global Communications Conference (GLOBECOM)*, 2016, pp. 1–6.

[15] G. S. Aujla, M. Singh, N. Kumar, and A. Zomaya, "Stackelberg Game for Energy-aware Resource Allocation to Sustain Data Centers Using RES," *IEEE Transactions on Cloud Computing*, 2017, doi: 10.1109/TCC.2017.2715817.

[16] A. C. L. Hernández, N. L. D. Aldana, M. Graells, J. C. V. Quintero, and J. M. Guerrero, "Mixed-Integer-Linear-Programming-Based Energy Management System for Hybrid PV-Wind-Battery Microgrids: Modeling, Design, and Experimental Verification," *IEEE Transactions on Power Electronics*, vol. 32, no. 4, pp. 2769–2783, 2017.

[17] P. Malysz, S. Sirouspour, and A. Emadi, "An optimal energy storage control strategy for grid-connected microgrids," *IEEE Transactions on Smart Grid*, vol. 5, no. 4, pp. 1785–1796, 2014.

[18] I. Sengor, H. C. Kilickiran, H. Akdemir, B. Kekezoglu, O. Erdinc, and J. P. Catalão, "Energy Management of A Smart Railway Station Considering Regenerative Braking and Stochastic Behaviour of ESS and PV Generation," *IEEE Transactions on Sustainable Energy*, 2017.

[19] L. Yao, J.-Y. Shen, and W. H. Lim, "Real-Time Energy Management Optimization for Smart Household," in *Internet of Things (iThings) and IEEE Green Computing and Communications (GreenCom) and IEEE Cyber, Physical and Social Computing (CPSCom) and IEEE Smart Data (SmartData), 2016 IEEE International Conference on*. IEEE, 2016, pp. 20–26.

[20] O. Erdinc, N. G. Paterakis, T. D. Mendes, A. G. Bakirtzis, and J. P. Catalão, "Smart household operation considering bi-directional EV and ESS utilization by real-time pricing-based DR," *IEEE Transactions on Smart Grid*, vol. 6, no. 3, pp. 1281–1291, 2015.

[21] Y. Wang, B. Wang, T. Zhang, H. Nazaripouya, C.-C. Chu, and R. Gadh, "Optimal energy management for Microgrid with stationary and mobile storages," in *Transmission and Distribution Conference and Exposition (T&D), 2016 IEEE/PES*. IEEE, 2016, pp. 1–5.

[22] D. Thomas, C. S. Ioakimidis, V. Klonari, F. Vallée, and O. Deblecker, "Effect of electric vehicles' optimal charging-discharging schedule on a building's electricity cost demand considering low voltage network constraints," in *PES Innovative Smart Grid Technologies Conference Europe (ISGT-Europe), 2016 IEEE*. IEEE, 2016, pp. 1–6.

[23] J. Tan and Y. Zhang, "Coordinated Control Strategy of a Battery Energy Storage System to Support a Wind Power Plant Providing Multi-Timescale Frequency Ancillary Services," *IEEE Transactions on Sustainable Energy*, 2017, doi: 10.1109/TSTE.2017.2663334.

[24] G. T. . V. (2012-09), "3rd Generation Partnership Project; Technical Specification Group Services and System Aspects; System improvements for Machine-Type Communications (MTC) (Release 11)," Tech. Rep.

[25] M. B. Shahab, A. Hussain, and M. Shoaib, "Smart grid traffic modeling and scheduling using 3gpp lte for efficient communication with reduced ran delays," in *Telecommunications and Signal Processing (TSP), 2013 36th International Conference on*. IEEE, 2013, pp. 263–267.

[26] G. D. Yalcin and N. Erginel, "Determining weights in multi-objective linear programming under fuzziness," in *Proceedings of the World Congress on Engineering*, vol. 2, 2011, pp. 6–8.

[27] X.-q. Li, B. Zhang, and H. Li, "Computing efficient solutions to fuzzy multiple objective linear programming problems," *Fuzzy sets and systems*, vol. 157, no. 10, pp. 1328–1332, 2006.

[28] I. Duggal and B. Venkatesh, "Short-term scheduling of thermal generators and battery storage with depth of discharge-based cost model," *IEEE Transactions on Power Systems*, vol. 30, no. 4, pp. 2110–2118, 2015.

[29] R. S. Zebulum, M. A. Pacheco, and M. M. B. Vellasco, *Evolutionary electronics: automatic design of electronic circuits and systems by genetic algorithms*. CRC press, 2001, vol. 22.

[30] "Mosek," [Accessed on: Apr. 2017]. [Online]. Available: https://www.mosek.com/resources/downloads

[31] PJM, "Regulation Signal Data - June 2014," [Accessed: Mar. 2017]. [Online]. Available: http://www.pjm.com/markets-and-operations/ancillary-services.aspx

[32] (2015, Jun.) 2014 annual report on market issues & performance. Department of Market Monitoring. California ISO. [Accessed on: Mar. 2017].